TU Delft

Delft University of Technology

Document Version
Final published version

Licence
Dutch Copyright Act (Article 25fa)

Citation (APA)
Zhou, S., Bruijn, J. D., Besseling, F., Metrikine, A., Dalen, K. V., & Steenbergen, M. (2026). Directivity of Train-Induced Ground Vibration & Measurement Insights. In Z. Dimitrovová, P. Biswas, & T. A. N. Silva (Eds.), *Proceedings of ICOVP and WMVC 2025 - Vibration Problems and Wave Mechanics: Insights and Innovations* (pp. 421-430). (Lecture Notes in Mechanical Engineering). Springer. https://doi.org/10.1007/978-3-032-11549-2_43

Important note
To cite this publication, please use the final published version (if applicable).
Please check the document version above.

Copyright
In case the licence states “Dutch Copyright Act (Article 25fa)”, this publication was made available Green Open Access via the TU Delft Institutional Repository pursuant to Dutch Copyright Act (Article 25fa, the Taverne amendment). This provision does not affect copyright ownership.
Unless copyright is transferred by contract or statute, it remains with the copyright holder.

Sharing and reuse
Other than for strictly personal use, it is not permitted to download, forward or distribute the text or part of it, without the consent of the author(s) and/or copyright holder(s), unless the work is under an open content license such as Creative Commons.

Takedown policy
Please contact us and provide details if you believe this document breaches copyrights.
We will remove access to the work immediately and investigate your claim.

This work is downloaded from Delft University of Technology.

Directivity of Train-Induced Ground Vibration & Measurement Insights

Sijia Zhou[1(✉)], Janno de Bruijn[2], Floris Besseling[2], Andrei Metrikine[1], Karel van Dalen[1], and Michaël Steenbergen[1]

[1] Delft University of Technology, 2628CN Delft, The Netherlands
S.Zhou-3@tudelft.nl
[2] Witteveen & Bos, 7411TJ Deventer, The Netherlands

Abstract. The study of train-track interaction and resulting ground vibrations generally (and often exclusively) focuses on the vertical direction. This study explores the directional characteristics of train-induced ground vibration, based on in-situ measurements conducted at different locations in the Netherlands with two subsoil types - sand and clay, and different substructures, for a set of operational parameters. Triaxial accelerometers were installed at the ground surface along the track, in a spatial configuration capturing both near-field (or non-radiating) and far-field (or radiating) contributions of the ground response in terms of particle motion. Through statistical and comparative analyses of field-measured data, the results show a strong dependence of the dominating directions of particle motion on the ground composition (soft or still soils) and therefore also on the cross-sectional track geometry in terms of substructure and embankment. These findings highlight the relevance of paying due attention to both normal and in-plane (longitudinal and lateral) components of train-track interaction and ground particle motion in the modeling, mitigation and prediction of train-induced vibration hindrance.

Keywords: Train-induced vibration · Vibration hindrance · Ground vibration · In-plane surface excitation · Particle motion · Acceleration measurement

1 Introduction

Ground vibrations induced by train traffic pose critical challenges in transportation engineering, particularly in relation to hindrance in residential areas. Thus, understanding the different sources of train-induced vibration is essential for mitigation.

While most of the existing research focuses on vertical vibration of the free surface in terms of particle motion, due to its direct association with axle loads [1, 2], lateral ground particle motion has received relatively less attention. Classical analytical approaches, such as one-dimensional (1-D) and two-dimensional (2-D) models based on beam-on-elastic-foundation theory, have provided valuable insights into simplified soil–structure interactions [3–5]. These models have their merits in the study of train-track interaction; they are however unsuitable for the analysis of lateral vibration and generally the response of the surface adjacent to the track.

© The Author(s), under exclusive license to Springer Nature Switzerland AG 2026
Z. Dimitrovová et al. (Eds.): ICOVP & WMVC 2025, LNME, pp. 421–430, 2026.
https://doi.org/10.1007/978-3-032-11549-2_43

To overcome these limitations, more advanced three-dimensional (3-D) models have been developed. Approaches such as equivalent stiffness method [6, 7], semi-analytical wave-based methods [8] and Finite Element method (FEM), provide improved spatial resolution and allow for more realistic representation of 3-D ground motion, radiation of mechanical energy and wave propagation[9, 10]. Only a limited number of models incorporate lateral loads and investigate the lateral response [11]. Their methods mainly rely on the equivalent stiffness method to describe load-half space interaction but have limitations in capturing complex train-track-soil interactions.

The wide and relatively cheap application of triaxial sensors in field monitoring, has allowed the development of extensive measurement configurations for near- and far-field surface vibrations capturing all three directions. Nonetheless, experimental studies incorporating a systematic directional analysis of particle motion in train-induced vibration remain an exemption [1, 12, 13].

This paper explores the role of lateral particle motion in train-induced surface vibration. Triaxial vibration data were systematically collected at two sites in the Netherlands, with sand and clay subsoil, and including both passenger and freight trains. By statistically analyzing the dominant particle motion direction at different sites and distances from the track, the study reveals the vibration directivity and highlights the significance of lateral components in the overall vibration field.

2 Measurement Setup

Field data were obtained from long-term vibration monitoring conducted at two railway sites in the Netherlands: Holten and Schalkwijk. The cross-sections profile of embankments and the sensor layout at both sites are further illustrated in Fig. 1.

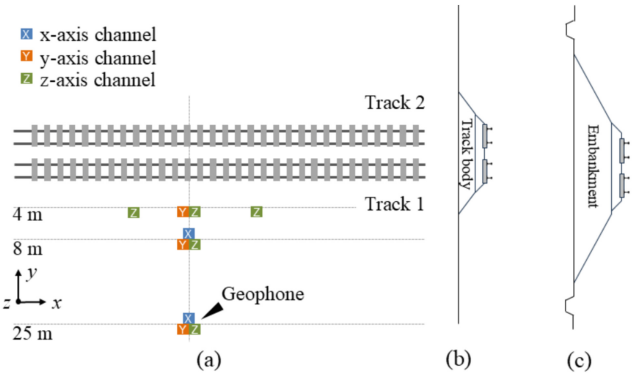


Fig. 1. Sensor layouts and embankment cross-sectional profiles at the Holten and Schalkwijk sites: (a) layout of the sensor arrays; (b) embankment cross-sectional profiles at Holten; (c) embankment cross-sectional profiles at Schalkwijk.

At the Holten site, the railway is constructed on sandy ground with a relatively low embankment. In contrast, the Schalkwijk site has a higher embankment built on soft

clay, accompanied by trenches along both sides serving drainage purposes. At each site, triaxial accelerometers and geophones were installed at distances of 4 m, 8 m and 25 m from Track 1. Typical configurations for each train type, including freight, Intercity, and Sprinter, are summarized in Fig. 2. Additionally, Fig. 3 presents the distribution of dead weight per axle, derived from field measurements.

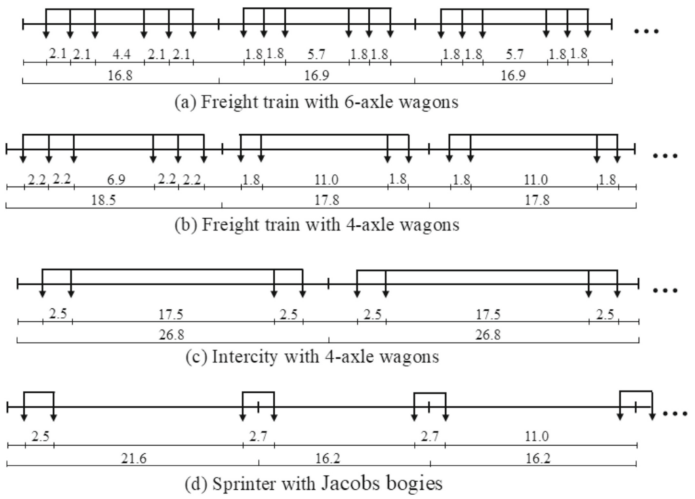


Fig. 2. Representative configurations of typical freight, Sprinter and Intercity trains.

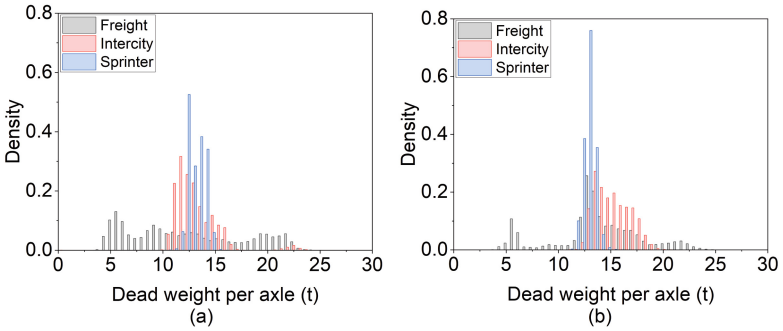


Fig. 3. Probability density distributions of dead weight per axle for different train type: (a) at the Holten site and (b) at the Schalkwijk sites.

Acceleration signals were first converted into velocities by time integration and then bandpass filtered within the frequency range of 1–315 Hz. For each train passage event, the maximum absolute velocity (v_{max}) in each direction (x, y and z) was separately identified as the peak value of the time-domain signal within a defined time window T, corresponding to the period during which the amplitude of the time signal exceeds

one-quarter of its maximum absolute value. This determination of v_{max} allows direct comparison of the relative contribution and directional characteristics of vibrations. Moreover, to evaluate the hindrance caused by train-induced vibrations to the surrounding environment, the highest v_{max} among all three directions for a given train passage value is generally used, reflecting the peak transient intensity.

In addition, the root mean square (RMS) velocity (vrms) in three directions was computed within the same time window T by Eq. 1, it represents the average intensity and is consistent with the physical interpretation of the directional components of kinetic energy.

$$v_{\mathrm{rms},i} = \sqrt{\frac{1}{T}\int_0^T [v_i(t)]^2 \mathrm{d}t} \tag{1}$$

where $v_{\mathrm{rms},i}$ denotes the root mean square velocity in direction i, (i = x, y, z), $v_i(t)$ is the velocity signal in that direction, and T is the duration of the train passage.

3 Results and Discussion

3.1 Directivity of Vibrations

Figure 4 and Fig. 5 illustrate the distribution of dominant vibration directions across different train types (freight, Intercity, and Sprinter) and distances (4 m, 8 m, 25 m) at the Holten and Schalkwijk sites, based on train passages on track 1. Track 1 was selected for detailed analysis as it is closer to the sensor array, enabling more effective registration of near-field vibration effects. In this study, dominance is defined as the number of events in which the v_{max} of a given direction (x, y, or z) is the highest among all three components for a given train passage.

At the Holten site, as shown in Fig. 4, the particle motion in y-direction exhibits strong dominance across most train types and distances, especially for freight. As illustrated by the cross-sectional profiles in Fig. 1, the embankment at this site is relatively low and built on sandy subsoil. The sensor at 4 m is installed near the toe of the embankment slope, where the geometric configuration and composition of track structures may contribute to an amplification of quasi-static lateral ground responses under train loads. When trains run on track 1, the axle loads act directly above the near-side slope, which is likely to induce significant lateral thrust on the embankment toe. These interactions could help explain the observed dominance of lateral vibration near the track. However, a clear distinction between radiating and non-radiating wave components to this near-field phenomenon has not been established and needs further investigation.

With increasing distance from the track, the quasi-static response is observed to decay rapidly, while the relative contribution of radiating wave components appears to be more significant. The sandy subsoil, characterized by low damping and high shear stiffness, is conducive to the long-distance propagation of surface waves with significant lateral components. As a result, lateral particle motion not only dominates in the near field but is also observed in the far field at 25 m, as observed in the measurement.

At Schalkwijk, in contrast, the dominant vibration direction in the near field (4 m and 8 m) is consistently vertical for all train types and both tracks. This phenomenon

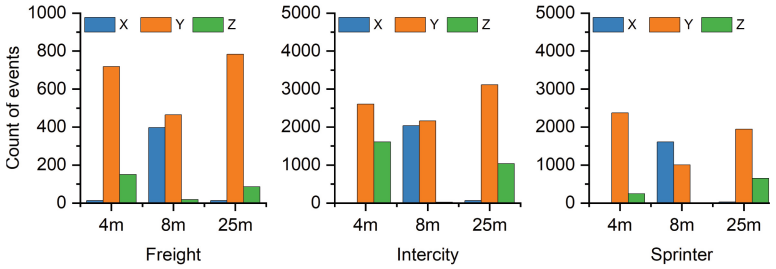


Fig. 4. Event count where v_{max} in x, y, or z direction is the largest among all components, at different distances from the track at the Holten site.

likely reflects the influence of the higher embankment and properties of clay subsoil. As illustrated in Fig. 1, sensors installed at 4 m and 8 m are positioned on the embankment slope. Compared to the soft subsoil, the embankment is much stiffer and is therefore expected to vibrate primarily vertically under train loads, thereby transmitting more energy in the vertical direction. As a result, the ground response in the near field is observed to be dominated by vertical motion, while lateral wave transmission appears to be significantly reduced.

At a greater distance of 25 m, however, lateral motion begins to rival or even exceed the vertical motion, particularly for Sprinter and Intercity trains. This phenomenon may be influenced by higher train speeds, which tend to induce more pronounced dynamic track excitation, thereby supporting the generation of radiating components. Additionally, differences in axle configurations, such as the distribution of driven and non-driven axles, and the potential for hunting oscillations, may further enhance lateral wave generation.

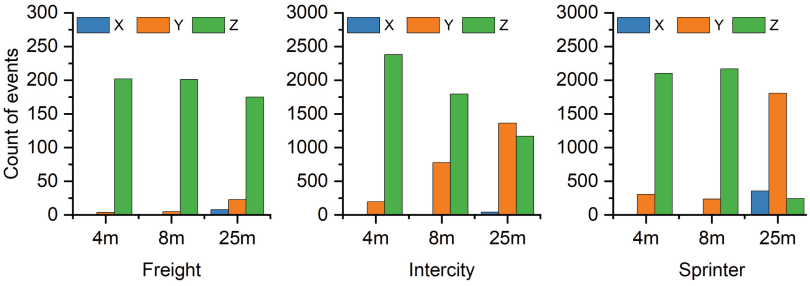


Fig. 5. Event count where Vmax in X, Y, or Z direction was the largest among all components, at different distances from the track at the Schalkwijk site.

3.2 Maximum Absolute Velocity Distribution and Directional Variability

Figure 6 and Fig. 7 present probability density distributions of v_{max} values for two representative train types—freight and Intercity—at Holten, corresponding to train passages on track 1.

At the Holten site, the v_{max} value in y-direction exhibits higher peaks and a broader distribution compared to the z-direction for both trains. Specifically, at the 4 m distance, the peak of the y-direction probability density distribution for freight is approximately 6.0 mm/s, with the distribution extending beyond 8 mm/s. In contrast, the peak for the z-direction is around 4.5 mm/s and primarily concentrated within the lower velocity range. Although the overall v_{max} amplitudes decrease with increasing distance, the y-direction peaks consistently remain higher across all distances. These observations indicate that the lateral motion is not only more frequently dominant in amplitude but also reaches higher peak values compared to the vertical motion.

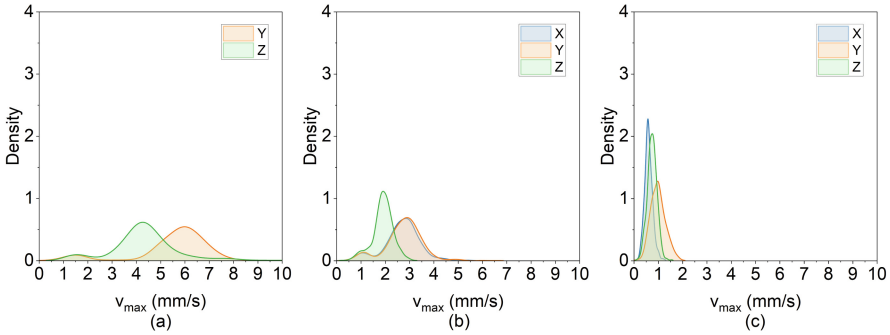


Fig. 6. Probability density distributions of the maximum velocity v_{max} of freight when trains running on track 1 at the Holten site at three distances: (a) 4 m; (b) 8 m and (c) 25 m.

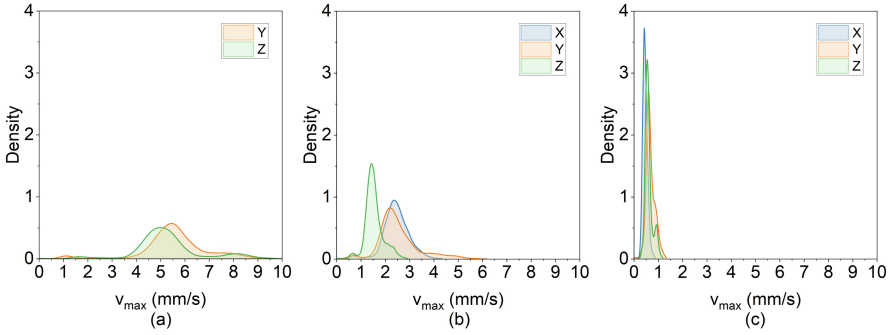


Fig. 7. Probability density distributions of the maximum velocity v_{max} of Intercity when trains running on track 1 at the Holten site at three distances: (a) 4 m; (b) 8 m and (c) 25 m.

Figure 8 and Fig. 9 illustrate the probability density distributions of v_{max} in three directions at Schalkwijk. In contrast to the observations at the Holten site, the difference between peaks of y- and z-direction at Schalkwijk is relatively small. Ground vibration in z-direction consistently exhibits the highest peak density values, particularly in the near-field at 4 m and 8 m. This may reflect the influence of embankment configuration at

this site, particularly the height and material, which are generally known to affect load transmission and attenuation.

However, at 25 m, the v_{max} in y-direction for Intercity trains generally becomes comparable to or slightly exceeds that in the z-direction. This directional shift is consistent with trends observed in dominance direction counts presented in Fig. 5. The pattern indicates an increasing relative contribution from radiating surface waves in the far field, potentially due to the decay of quasi-static effect and excited surface waves that contribute to lateral particle motions become more prominent. A full explanation for this phenomenon requires further investigation.

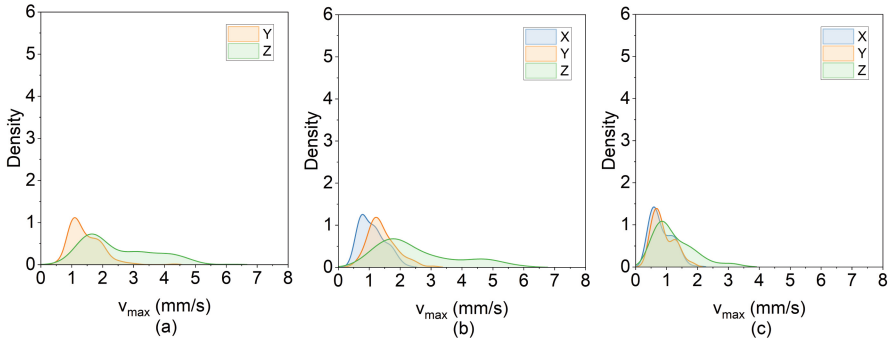


Fig. 8. Probability density distributions of the maximum velocity v_{max} of freight when trains running on track 1 at the Schalkwijk site at three distances: (a) 4 m; (b) 8 m and (c) 25 m.

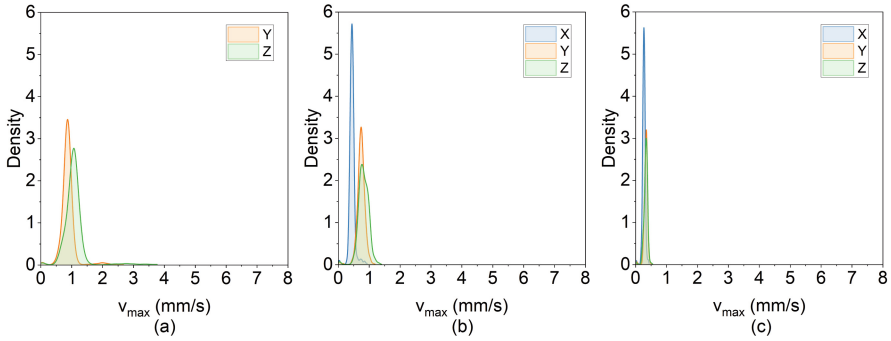


Fig. 9. Probability density distributions of the maximum velocity v_{max} of Intercity when trains running on track 1 at the Schalkwijk site at three distances: (a) 4 m; (b) 8 m and (c) 25 m.

3.3 RMS Velocity Distribution and Directional Variability

Figure 10 presents the probability density distributions of v_{rms} values in y- and z-directions at the Holten site for freight and Intercity trains passing through Track 1 at three distances.

For both train types, the peak of v_{rms} distribution is consistently higher in the y-direction across all distances. Specifically, at 4 m, the peak v_{rms} value in y-direction is

approximately 0.9 mm/s, while that in z-direction is around 0.6 mm/s. indicates that lateral vibrations contribute more substantially to the average kinetic energy of particle motions than vertical vibrations. In addition, the overall v_{rms} value for Intercity trains is lower than that for freight train, which likely results from the lower axle loads of Intercity trains.

The sustained higher average energy of lateral vibrations, even at longer distances, reflects that the sandy soil embankment at the Holten site may facilitate efficient transmission of lateral vibration energy induced by the train load.

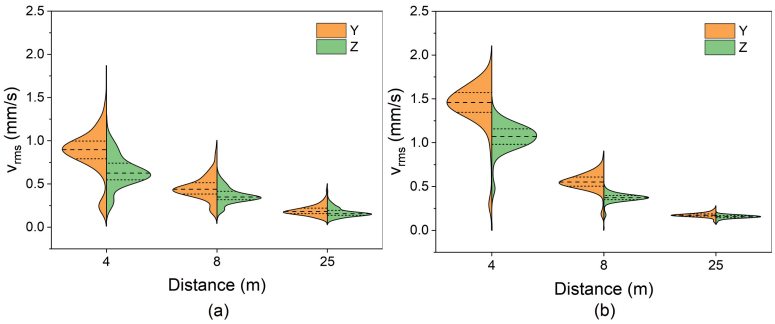


Fig. 10. Comparison of RMS velocity for lateral and vertical vibrations when trains running on track 1 at the Holten site: (a) freight; (b) Intercity.

As shown in Fig. 11a, the v_{rms} value of freight trains at Schalkwijk is generally the highest in the z-direction, in contrast to that at the Holten site, indicating a more substantial contribution of vertical vibrations to the average vibration energy.

For the Intercity train (Fig. 11b), the v_{rms} value in the y- and z-directions are approximately equal, with the y-direction showing slightly higher values at the far field. Notably, while the statistics in Fig. 5 show that lateral (y-direction) vibrations are more frequently identified as the dominant direction at 25 m, v_{rms} values reveal that the average energy in the y- and z-directions at this distance remains nearly equivalent.

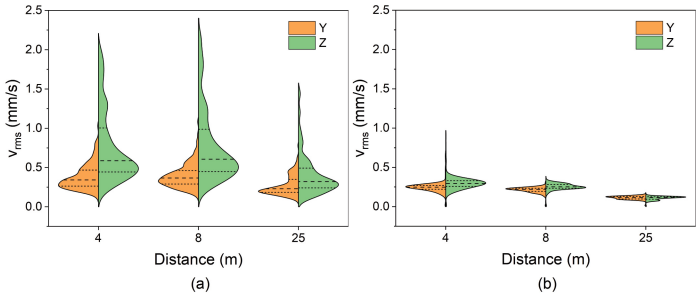


Fig. 11. Comparison of RMS velocity for lateral and vertical vibrations when trains running on track 1 at the Schalkwijk site: (a) freight; (b) Intercity.

3.4 Discussion

This study provides evidence that lateral ground surface motion is a significant component of train-induced ground vibrations, particularly on sandy ground and at greater distances from the track. The lateral dominance is likely influenced by multiple factors, including subsoil properties, substructure geometry, wave attenuation characteristics and the decay of quasi-static components. In addition, the potential role of lateral force components generated at the wheel–rail interface warrants further investigation.

Future research will focus on further exploring the underlying physical mechanisms of these phenomena, particularly the effects of substructure geometry and characteristics of wave propagation and attenuation. This will also involve separating and quantifying the contribution of different wave types, such as Rayleigh, Love, and body waves, to both the near-field and far-field vibrations.

4 Conclusions

This study has provided a measurement-based insight into the directional characteristics of train-induced ground vibration. The results reveal that the lateral (y-direction) vibration frequently plays a significant role. Moreover, the directivity of train-induced ground vibrations is not only determined by distance but also depends on subsoil characteristics and the presence and geometry of a railway embankment.

At sandy sites without embankment (Holten), lateral vibration dominance is observed across a wide range of distances. In contrast, at clay subsoil sites (Schalkwijk), vertical dominance remains prominent in the near field, the stiff embankment structure and the higher damping characteristics of clay likely promote efficient vertical transmission of train loads while limiting the development of lateral wave components. Although lateral dominance emerges at greater distances, the trend is less pronounced than at the sandy site.

These findings highlight the necessity of accounting for the in-plane ground surface vibrations. A more comprehensive understanding of vibration directionality is essential for improving prediction models and developing more effective vibration mitigation strategies.

References

1. Lombaert, G., Degrande, G., Kogut, J., François, S.: The experimental validation of a numerical model for the prediction of railway induced vibrations. J. Sound Vib. **297**, 512–535 (2006). https://doi.org/10.1016/j.jsv.2006.03.048
2. Gao, G., Chen, J., Song, J., Yang, J., Yao, S.: Field measurement and analysis of ground vibration induced by high-speed train. In: Bian, X., Chen, Y., and Ye, X. (eds.) Environmental Vibrations and Transportation Geodynamics. pp. 119–132. Springer Singapore, Singapore (2018). https://doi.org/10.1007/978-981-10-4508-0_11
3. Fărăgău, A.B., Metrikine, A.V., Van Dalen, K.N.: Transition radiation in a piecewise-linear and infinite one-dimensional structure–a Laplace transform method. Nonlinear Dyn. **98**, 2435–2461 (2019). https://doi.org/10.1007/s11071-019-05083-6

4. Van Dalen, K.N., Tsouvalas, A., Metrikine, A.V., Hoving, J.S.: Transition radiation excited by a surface load that moves over the interface of two elastic layers. Int. J. Solids Struct. **73–74**, 99–112 (2015). https://doi.org/10.1016/j.ijsolstr.2015.07.001
5. Dimitrovová, Z., Biswas, P., Gonçalves, R., Silva, T. (eds.): Recent Trends in Wave Mechanics and Vibrations: Proceedings of WMVC 2022. Springer International Publishing, Cham (2023). https://doi.org/10.1007/978-3-031-15758-5
6. Dieterman, H.A., Metrikine, A.: Equivalent stiffness of a half-space interacting with a beam. critical velocities of a moving load along the beam. Eur. J. Mech. ASolids. **15**, 67–90 (1996)
7. Steenbergen, M.J.M.M., Metrikine, A.V.: The effect of the interface conditions on the dynamic response of a beam on a half-space to a moving load. Eur. J. Mech. - ASolids. **26**, 33–54 (2007). https://doi.org/10.1016/j.euromechsol.2006.03.003
8. Ba, Z., Liang, J., Lee, V.W., Gao, Y.: A semi-analytical method for vibrations of a layered transversely isotropic ground-track system due to moving train loads. Soil Dyn. Earthq. Eng. **121**, 25–39 (2019). https://doi.org/10.1016/j.soildyn.2019.02.019
9. Hu, J., Bian, X.: Analysis of dynamic stresses in ballasted railway track due to train passages at high speeds. J. Zhejiang Univ.-Sci. A. **23**, 443–457 (2022). https://doi.org/10.1631/jzus.A2100305
10. Correia Dos Santos, N., Barbosa, J., Calçada, R., Delgado, R.: Track-ground vibrations induced by railway traffic: experimental validation of a 3D numerical model. Soil Dyn. Earthq. Eng. **97**, 324–344 (2017). https://doi.org/10.1016/j.soildyn.2017.03.004
11. Metrikine, A.V., Dieterman, H.A.: Three-dimensional vibrations of a beam on an elastic half-space: resonance interaction of vertical-longitudinal and lateral beam waves. J. Appl. Mech. **64**, 951–956 (1997). https://doi.org/10.1115/1.2789005
12. Wang, C., Lei, X., Liu, W., Si, P.: Prediction method of ground vibration caused by high-speed railway based on the formula from the federal transportation administration. J. Transp. Eng. Part Syst. **149**, 04023090 (2023). https://doi.org/10.1061/JTEPBS.TEENG-7859
13. Alves Costa, P., Calçada, R., Silva Cardoso, A.: Track–ground vibrations induced by railway traffic: in-situ measurements and validation of a 2.5D FEM-BEM model. Soil Dyn. Earthq. Eng. **32**, 111–128 (2012). https://doi.org/10.1016/j.soildyn.2011.09.002